

Unconventional Superfluidity in a model of Fermi-Bose Mixtures

K Sheshadri^{1,*} and A Chainani^{2,†}

¹*226, Bagalur, Bangalore North, Karnataka State, India 562149 and*

²*Condensed Matter Physics Group, National Synchrotron Radiation Research Center, Hsinchu 30076, Taiwan*

(Dated: December 8, 2021)

A finite-temperature ($T > 0$) study of a model of a mixture of spin-zero hardcore bosons and spinless fermions, with filling fractions ρ_B and ρ_F , respectively, on a two-dimensional square lattice with composite hopping t is presented. The composite hopping swaps the locations of a fermion and a boson that occupy nearest-neighbor sites of the lattice. The superfluid order parameter ψ , the fermion hopping amplitude ϕ , the chemical potential μ , the free energy minimum \bar{F} and entropy S are calculated in the limit $\rho_B + \rho_F = 1$ within a mean-field approximation, and lead to a phase diagram in the $\rho_F - T$ plane. This phase diagram consists of a metallic superfluid phase under a dome-shaped $T(\rho_F)$, and insulating normal liquid and insulating normal gas phases outside the dome. These phases are separated by coupled discontinuous transitions as indicated by jumps in ψ and ϕ . The maximum critical transition temperature T_c is observed very close to $\rho_F = 1/2$. While $\bar{F}(T)$ is continuous with a derivative discontinuity at $T = T_c(\rho_F)$ for $0 < \rho_F \leq 1/2$ (first-order transition), it becomes *discontinuous* for $\rho_F > 1/2$ (zeroth-order transition), where the entropy becomes negative for a range of temperatures below T_c . The ratio of T_c to Fermi band width agrees remarkably with the ratio of T_c/T_F (where T_F is the Fermi temperature) of unconventional superfluids and superconductors like Fermi-Bose mixtures, the high- T_c cuprates, iron-based and hydride superconductors, that exhibit experimental values of T_c spread over nine orders of magnitude from $\sim 200\text{nK}$ to $\sim 260\text{K}$.

I. INTRODUCTION

Fermi-Bose mixtures (FBMs) constitute an unusual and important state of matter, including well known examples like He³-He⁴ mixtures¹, the mixed phase of type-II superconductors, ultracold atom systems²⁻⁴, unconventional superconductors which exhibit Bardeen-Cooper-Schrieffer to Bose-Einstein condensation (BCS-BEC) crossover⁵⁻⁸, and so on. Experimental and theoretical studies of FBMs have shown remarkable results, particularly in terms of the BCS-BEC crossover across a Feshbach resonance⁹, that have revealed their distinct aspects compared to the limiting cases of BCS superconductivity and BEC superfluidity^{10,11}.

The BCS-BEC crossover was originally predicted to occur for excitons in semiconductors¹² and quarks in high energy physics¹³. However, it was first reported experimentally in ultracold fermionic atoms with s-wave interactions¹⁴. Unusual and unexpected results include formation of a Feshbach molecule¹⁵, and the role of three body physics¹⁶ in FBMs. On the other hand, the role of BCS-BEC crossover in condensed matter involves experimental results on iron-based superconductors⁵⁻⁸ and its relation to well-accepted theoretical results^{10,17,18}. While interactions between fermions mediated by phonons define the BCS theory of superconductivity, several studies have also considered their importance in mixtures of ultracold atoms¹⁹⁻²². The Boson-Fermion (BF) model²³, which preceded the BCS theory, discusses itinerant fermions hybridizing with bosons composed of bound pairs of fermions of opposite spins. The BF model was subsequently used to study electrons interacting with local lattice deformations²⁴ as well as high temperature superconductivity²⁵⁻²⁸. Recent studies have ap-

plied it for describing resonance superfluids in the BCS-BEC crossover regime²⁹, as well as a temperature driven crossover in an FBM³⁰. These studies have shown the importance and interplay of bosonic and fermionic degrees of freedom in various physical systems.

Early studies on mixtures investigated the role of an attractive interaction between fermions and bosons. It was shown that an FBM with attractive interactions undergoes a collapse when the fermion number exceeded a critical value³¹. The breakthrough in controlling a Feshbach resonance in FBMs allowed researchers to effectively tune the boson-fermion interaction and control the system from collapsing at high densities³². In contrast, theoretical studies employing repulsive interactions could describe various stable density configurations of FBMs. The role of finite temperatures and going beyond the mean-field approximation was also investigated²². In the case of a strongly repulsive quasi one-dimensional FBM,³³ it was shown that the phase diagram as a function of applied magnetic field H displays a pure boson phase for $H = 0$, polarized fermions and bosons coexisting for $0 < H < H_c$, and a fully polarized fermion phase for $H > H_c$. More interestingly, for an FBM on a 2D optical lattice in the framework of an extended single band Hubbard model with Coulomb interaction terms between bosons (U_{BB}), between fermions (U_{FF}) and an additional Coulomb interaction between bosons and fermions (U_{BF}), it was shown that the bosons can mediate an attractive interaction between fermions, leading to fermion paired states with different s , p and d orbital symmetries³⁴. Further, the phase diagram as a function of U_{BF} versus fermion number also revealed the existence of spin density wave and charge density wave phases. The authors also predicted that for experimentally accessible regime of parameters, the 2D

FBM would exhibit superfluidity with an unconventional fermion pairing having a transition temperature around a percent of the Fermi energy. On the other hand, the role of interaction-dependent temperature effects in an FBM were investigated by Cramer³⁵. It was shown that adiabatic temperature changes of the FBM occur which depend on the interaction between fermions and bosons³⁵.

In addition, the dynamics of FBMs has also been investigated and it was shown that long range density wave phases can be obtained for fermions and bosons hopping independently in the presence of on-site boson-boson U_{BB} and boson-fermion U_{BF} Coulomb interactions^{36,37}. However, a *composite* hopping that exchanges a fermion with a boson, when they occupy neighboring sites, was not considered in earlier work. This form of hopping was proposed recently by us^{38,39} and distinguishes our work from earlier work on FBMs. In this work, we calculate the thermodynamic properties of a model of FBM on a two-dimensional square lattice with composite hopping between neighboring spinless fermions and hardcore bosons, extending our earlier study of $T = 0$ properties^{38,39}. As in the previous work, we use a mean-field approximation and restrict ourselves to the case

$$\rho_F + \rho_B = 1, \quad (1)$$

where ρ_F and ρ_B are the filling fractions of the fermions and bosons, respectively. To recall, at $T = 0$, the model displays two distinct phases separated by *coupled first-order* transitions at Fermi filling fraction $\rho_F \simeq 0.3$: for $\rho_F < 0.3$ the Fermi sector is insulating and the Bose sector is a normal liquid, while for $\rho_F > 0.3$ the Fermi sector is metallic and the Bose sector is a superfluid. In the present work, we find that thermal fluctuations suppress superfluidity, and at a certain $T = T_c(\rho_F)$ there is a discontinuous transition to an insulating non-superfluid phase as shown by the superfluid amplitude $\psi(T)$ and the fermion hopping amplitude $\phi(T)$. We further find that the transition occurring at $T_c(\rho_F)$ is first order for $0.3 < \rho_F \leq 1/2$ (the minimum free energy $\tilde{F}(T)$ is continuous with a discontinuity in its first derivative), but is zeroth order for $1/2 < \rho_F < 1$ (the minimum free energy $\tilde{F}(T)$ is discontinuous). In the latter regime, the entropy becomes *negative* for a range of temperatures below T_c . We compute the ratio of T_c to the Fermi band width, and find remarkable agreement with measured values in the range of 0.02 to 0.20 for a wide variety of unconventional superfluids and superconductors, including Fermi-Bose mixtures, the high- T_c cuprates, iron-based superconductors and hydrides, that have their T_c spread over nine orders of magnitude from a few hundred nanokelvins to a few hundred kelvins³⁹. Our estimate for the superconducting T_c in the solid-state context with known experimental band widths or the Fermi temperature are consistent with observed T_c 's of the cuprates as well as iron-based superconductors.

II. THE COMPOSITE-HOPPING MODEL AND ITS MEAN-FIELD THERMODYNAMICS

We consider the composite-hopping model with Hamiltonian

$$H = -\alpha \sum_i \left[b_i^\dagger b_i + f_i^\dagger f_i - 1 \right] - \mu \sum_i f_i^\dagger f_i - t \sum_{\langle ij \rangle} f_i^\dagger f_j b_j^\dagger b_i \quad (2)$$

that was proposed in a recent study for $T = 0$ ^{38,39}, where the notation used above is also explained. In this work also, we consider a FBM on a two-dimensional square lattice. The composite hopping term, the last term above, results in swapping of a hardcore boson and a spinless fermion when they occupy nearest-neighbor sites. Using the mean-field approximation, this term is transformed according to

$$f_i^\dagger f_j b_j^\dagger b_i \simeq \langle f_i^\dagger f_j \rangle (\langle b_j^\dagger \rangle b_i + \langle b_i \rangle b_j^\dagger - \langle b_j^\dagger \rangle \langle b_i \rangle) + \langle b_j^\dagger \rangle \langle b_i \rangle f_i^\dagger f_j - \langle f_i^\dagger f_j \rangle \langle b_j^\dagger \rangle \langle b_i \rangle, \quad (3)$$

so H is approximated by a mean-field Hamiltonian

$$\begin{aligned} H^{MF} &= H_0 + H_1 + H_2, \quad \text{where} \\ H_0 &= N(2\phi\psi^2 + \alpha), \\ H_1 &= -(\alpha + \mu) \sum_i f_i^\dagger f_i - \frac{1}{z} \psi^2 \sum_{\langle ij \rangle} f_i^\dagger f_j, \quad \text{and} \\ H_2 &= \sum_i \left[-\alpha b_i^\dagger b_i - \phi\psi(b_i + b_i^\dagger) \right]. \end{aligned} \quad (4)$$

We have taken $zt = 1$ (z is the coordination number of the lattice), and introduced the thermodynamic expectation values

$$\phi = \langle f_i^\dagger f_j \rangle, \quad \psi = \langle b_i \rangle = \langle b_j^\dagger \rangle. \quad (5)$$

We assume ϕ and ψ to be real and homogeneous and consider ψ to be the superfluid order parameter⁴⁰⁻⁴⁶. For the hardcore bosons, we use the single-site boson occupation number basis $\{|0\rangle, |1\rangle\}$ for diagonalizing the 2×2 matrix h_2 of H_2/N , i.e.,

$$h_2 = \begin{bmatrix} 0 & -\phi\psi \\ -\phi\psi & -\alpha \end{bmatrix} \quad (6)$$

that has the eigenvalues

$$\lambda_{\pm} = \frac{1}{2} [-\alpha \pm R], \quad \text{where } R = \sqrt{\alpha^2 + 4\phi^2\psi^2}. \quad (7)$$

Using the Fourier transform

$$f_i = \frac{1}{\sqrt{N}} \sum_{\mathbf{k}} e^{i\mathbf{k}\cdot\mathbf{r}_i} f_{\mathbf{k}}, \quad (8)$$

the Hamiltonian H_1 of the fermion sector becomes

$$H_1 = \sum_{\mathbf{k}} (\varepsilon_{\mathbf{k}} - \mu) f_{\mathbf{k}}^\dagger f_{\mathbf{k}}, \quad (9)$$

where

$$\begin{aligned}\varepsilon_{\mathbf{k}} &= -\alpha - \psi^2 \gamma_{\mathbf{k}}, \text{ and} \\ \gamma_{\mathbf{k}} &= \frac{2}{z}(\cos k_x + \cos k_y).\end{aligned}\quad (10)$$

The free energy per lattice site $F = F(\alpha, \psi)$ is now

$$\begin{aligned}F &= \frac{1}{2}(\alpha - R) + 2\phi\psi^2 - T \ln(1 + e^{-R/T}) \\ &\quad - T \frac{1}{N} \sum_{\mathbf{k}} \ln \left[1 + e^{(\mu - \varepsilon_{\mathbf{k}})/T} \right].\end{aligned}\quad (11)$$

We take $k_B = 1$ here and in the following. To calculate $\phi = \phi(\alpha, \psi)$, we use its definition in (5) and go over to k -space to get

$$\phi = \frac{1}{Nz} \sum_{\langle ij \rangle} \langle f_i^\dagger f_j \rangle = \frac{1}{N} \sum_{\mathbf{k}} \gamma_{\mathbf{k}} \langle f_{\mathbf{k}}^\dagger f_{\mathbf{k}} \rangle. \quad (12)$$

By definition,

$$\langle f_{\mathbf{k}}^\dagger f_{\mathbf{k}} \rangle = \frac{\text{Tr}(f_{\mathbf{k}}^\dagger f_{\mathbf{k}} e^{-H_1/T})}{\text{Tr}(e^{-H_1/T})} = \frac{1}{1 + e^{(\varepsilon_{\mathbf{k}} - \mu)/T}}, \quad (13)$$

and so

$$\phi = \frac{1}{N} \sum_{\mathbf{k}} \frac{\gamma_{\mathbf{k}}}{1 + e^{(\varepsilon_{\mathbf{k}} - \mu)/T}}. \quad (14)$$

Using $\gamma_{\mathbf{k}} = -(\alpha + \varepsilon_{\mathbf{k}})/\psi^2$ (the first equation in (10)) we obtain

$$\phi = -\frac{1}{N} \sum_{\mathbf{k}} \frac{\alpha + \varepsilon_{\mathbf{k}}}{\psi^2} \frac{1}{1 + e^{(\varepsilon_{\mathbf{k}} - \mu)/T}}. \quad (15)$$

Introducing the density of states

$$\rho(E) = \frac{1}{N} \sum_{\mathbf{k}} \delta(E - \varepsilon_{\mathbf{k}}), \quad (16)$$

we can write

$$\phi = -\frac{1}{\psi^2} \int_{E_0}^{\mu} dE \frac{\alpha + E}{1 + e^{(E - \mu)/T}} \rho(E), \quad (17)$$

where μ is chosen such that the fermion filling fraction

$$\rho_F(\alpha, \psi) = \int_{E_0}^{\mu} dE \frac{1}{1 + e^{(E - \mu)/T}} \rho(E) \quad (18)$$

has a desired value. Here, $E_0 = -\alpha - \psi^2$ is the minimum value of fermion energy. To calculate the density of states (16), we convert the k -sum in to an integral according to $(1/N) \sum_{\mathbf{k}} \rightarrow (1/4\pi^2) \int d\mathbf{k}$. Since $\varepsilon_{-\mathbf{k}} = \varepsilon_{\mathbf{k}}$, the k -space integral is four times the integral over the first quadrant of the Brillouin zone, and so we have

$$\rho(E) = \frac{1}{\pi^2} \int_0^\pi dk_x \int_0^\pi dk_y \delta(E + \alpha + \psi^2 \gamma_{\mathbf{k}}). \quad (19)$$

The integral over k_y can be easily evaluated, and we get

$$\begin{aligned}\rho(E) &= \frac{2}{\pi^2 \psi^2} f\left(\frac{\alpha + E}{\psi^2}\right), \text{ where} \\ f(u) &= \int_0^\pi \frac{dk_x}{\sqrt{1 - (2u + \cos k_x)^2}}.\end{aligned}\quad (20)$$

We can readily see that the function $f(u)$ is real only when $-1 \leq u \leq 1$, and is non-negative. Therefore we have the inequality $-\alpha - \psi^2 \leq E \leq -\alpha + \psi^2$ for the fermion energy E . We substitute the above expression for $\rho(E)$ in to equations (17) and (18) and transform the integrals to obtain

$$\begin{aligned}\rho_F &= \frac{2}{\pi^2} \int_{-1}^{u_F} du \frac{f(u)}{1 + e^{(u - u_F)\psi^2/T}} \text{ and} \\ \phi &= -\frac{2}{\pi^2} \int_{-1}^{u_F} du \frac{uf(u)}{1 + e^{(u - u_F)\psi^2/T}},\end{aligned}\quad (21)$$

where $u_F = (\alpha + \mu)/\psi^2$. This helps us choose the value of μ for a desired ρ_F , given the values of (α, ψ) . For any (ρ_F, T) , we determine ψ and α by solving $\partial F/\partial \psi = 0$ and $\partial F/\partial \alpha = 0$ simultaneously. These two equations, and the two equations in (21) above, are solved iteratively to obtain (α, ψ) as well as (ϕ, μ) for any chosen (ρ_F, T) . In general, there could be multiple solutions (α, ψ) . We substitute each solution in $F(\alpha, \psi)$ and denote the resulting free energy minimum for the solution by \tilde{F} ; the correct solution is the one that corresponds to the lowest \tilde{F} . From equation (11), we obtain

$$\begin{aligned}\frac{\partial F}{\partial \psi} &= 2\psi(\phi + \phi_\psi\psi) \left[1 - \frac{\phi}{R}\chi \right], \text{ and} \\ \frac{\partial F}{\partial \alpha} &= \frac{1}{2} \left[(1 - 2\rho_F) - \frac{\chi}{R}\alpha \right] + 2\phi_\alpha\psi^2 \left[1 - \frac{\chi}{R}\phi \right],\end{aligned}\quad (22)$$

where $\phi_\psi = \partial\phi/\partial\psi$, $\phi_\alpha = \partial\phi/\partial\alpha$, and

$$\chi(R, T) = \frac{e^{R/T} - 1}{e^{R/T} + 1}. \quad (23)$$

Since ϕ and ϕ_ψ are positive (see equations (14) and (21)), we always have $\phi + \phi_\psi\psi > 0$, so $\partial F/\partial \psi = 0$ gives

$$\psi = 0 \text{ or } R = \phi\chi(R, T). \quad (24)$$

Using this in equation (22), $\partial F/\partial \alpha = 0$ gives

$$\alpha = (1 - 2\rho_F)R/\chi. \quad (25)$$

III. TRACTABLE LIMITS AND SOME GENERAL OBSERVATIONS

Now that we have derived the implicit equations for ψ and α , we first analyze two simple limits: the $\psi = 0$ (disordered phase) and the $T = 0$ limits. We obtain

closed-form solutions for α , ψ and \tilde{F} in these limits. For the general case, we make some observations before moving on to a discussion of the numerical results in the next section.

From equation (25), we get $\alpha^2[\chi^2 - (1 - 2\rho_F)^2] = 4\phi^2\psi^2(1 - 2\rho_F)^2$. The solution $\psi = 0$ corresponds to the disordered state, i.e., the Bose sector is in a non-superfluid, normal phase. We then get $\alpha = 0$ or $\chi = |1 - 2\rho_F|$. In this state, $R = |\alpha|$, so using the definition of χ in equation (23) we get

$$\alpha = 0, T[\ln(1 - \rho_F) - \ln \rho_F] \quad (26)$$

in the disordered state ($\psi = 0$). Of these two solutions for α , we must pick the one corresponding to the lower \tilde{F} . Substituting the above in equation (11) for F , we obtain $\tilde{F}_I = -T(\ln 2)$ for the first solution $\alpha = 0$, and $\tilde{F}_{II} = -T[\ln 2 - \ln(1 - \rho_F)]$ for the second solution $\alpha = T[\ln(1 - \rho_F) - \ln \rho_F]$. We can see that $\tilde{F}_I < \tilde{F}_{II}$ for $\rho_F < 1/2$ and $\tilde{F}_{II} < \tilde{F}_I$ for $\rho_F > 1/2$. This shows that in the disordered phase, $\alpha = 0$ for $\rho_F \leq 1/2$ and $\alpha = T[\ln(1 - \rho_F) - \ln \rho_F]$ (which is the same as $\chi = |1 - 2\rho_F|$) for $\rho_F > 1/2$. In Fig. (1) we show the behavior of $-\tilde{F}_D/T$ (which is the disordered-phase entropy S_D) as a function of ρ_F .

At $T = 0$, we get $\tilde{F} = 0$ for the disordered state (since both \tilde{F}_I and \tilde{F}_{II} vanish). For the ordered state, $\chi = 1$ so that

$$\psi_0^2 = \rho_F(1 - \rho_F), \quad \alpha_0 = (1 - 2\rho_F)\phi_0, \quad (27)$$

and the minimum free energy is $\tilde{F}_0 = \rho_F^2[-\phi_0 + u_F(\rho_F - 1)]$ by taking the $T \rightarrow 0$ limit in equation (11) and substituting the above expressions for ψ_0 , α_0 . Here ψ_0 , ϕ_0 , α_0 and \tilde{F}_0 are $T = 0$ values. This gives coupled first-order transitions at $\rho_F \simeq 0.3$ at $T = 0$ between a metallic superfluid for $\rho_F > 0.3$ and an insulating normal liquid for $\rho_F \leq 0.3$. We referred to the latter as insulating normal gas in our earlier work^{38,39}. However, since the destruction of superfluidity of the Bose sector in this regime is due to an interplay between correlation and quantum effects and not due to temperature, this unusual phase should be more appropriately called an insulating normal liquid rather than an insulating normal gas.

As we increase the temperature at a fixed ρ_F , thermal fluctuations suppress superfluidity, reducing ψ . To see how this happens, we rewrite the ordered-phase self consistency equation $R = \phi\chi$ in the form $T = J(\psi)$ where $J(\psi) = \phi x / \ln[(1+x)/(1-x)]$; here $x = \sqrt{(1 - 2\rho_F)^2 + 4\psi^2}$. The function $J(\psi)$ has zeros at $\psi = 0$ (when $\phi = 0$) and $\psi = \psi_0$ (when $x = 1$). Since it is positive, it must have a maximum in the interval $(0, \psi_0)$. This is graphically illustrated in Fig. (2). As T increases from zero, the line $y = T$ intersects the curve $y = J(\psi)$ at two points $\psi = \psi_1, \psi_2$. Since $J(\psi)$ is a single-valued function, we have $\psi_2 < \psi_1 < \psi_0$ and further, ψ_1 decreases and ψ_2 increases as T is increased. The solution $\psi = \psi_1$ corresponds to the ordered minimum of the free

energy. As the temperature increases further, $y = T$ increases, while the maximum of $J(\psi)$ decreases, and at a certain temperature $T_2(\rho_F)$, the line $y = T$ becomes a tangent to $y = J(\psi)$ at the maximum, when $\psi_1 = \psi_2$. For $T > T_2(\rho_F)$, the self consistency equation $T = J(\psi)$ has no solution, and therefore $T_c \leq T_2$.

For $T \leq T_2$, when the ordered solution exists, there are two possibilities. (1) The ordered free energy minimum (\tilde{F}_O) remains lower than the disordered free energy minimum (\tilde{F}_D) for all $T \leq T_2$. In this case the transition temperature is $T_c = T_2$, and occurs when the ordered minimum ceases to exist. The free energy minimum value is discontinuous at the transition, since the system switches to the only solution that exists, namely $\psi = 0$. This corresponds to a *zeroth-order* transition. A zeroth-order phase transition has previously been considered in the theory of superfluidity and superconductivity⁴⁷. More recently, the reentrant phase transition in black holes has been discussed as a zeroth-order transition.⁴⁸⁻⁵³

Our numerical computations obtain this scenario for $\rho_F > 1/2$. (2) There exists a certain temperature $T_1 < T_2$ such that $\tilde{F}_O < \tilde{F}_D$ for $T < T_1$, and $\tilde{F}_O > \tilde{F}_D$ for $T > T_1$, with the two phases coexisting at $T_c = T_1$, which is a point of *first-order* transition. Our numerical results obtain this result for $\rho_F \leq 1/2$.

We can show that the transition is indeed zeroth order for $\rho_F > 1/2$ based on the disordered-phase behavior of α that we derived above. Formally, the solution of the self-consistency equation $R = \phi\chi$ is $\psi^2 = (1/4)[\chi^2 - (1 - 2\rho_F)^2]$. As we saw above, $\chi = |1 - 2\rho_F|$ in the disordered phase when $\rho_F > 1/2$, so the ordered solution $\psi > 0$ does not exist in the disordered phase. If $T_c < T_2$, then we would have the ordered solution existing in the disordered phase for $T_c < T < T_2$, which is a contradiction. So we must have $T_c = T_2$ in this case, resulting in a zeroth-order transition.

For $\rho_F \leq 1/2$, however, the ordered-phase self-consistency equation in the disordered phase (where $\alpha = 0$) becomes $2\psi = (e^{2\phi\psi/T} - 1)/(e^{2\phi\psi/T} + 1)$, that has a finite ψ solution for $T < T_2$. If $T_c = T_2$, then we would have an ordered solution existing in the disordered phase for $T > T_c = T_2$, a contradiction. We therefore have $T_c < T_2$ in this case. The transition criterion in this case is clearly $\tilde{F}_O = \tilde{F}_D$ since the ordered and disordered minima both exist at the transition. The transition for $\rho_F \leq 1/2$ is therefore first order.

We now turn to the correlation function $C(\mathbf{r}) = (1/N) \sum_i \langle \delta\rho_{\mathbf{r}_i} \delta\rho_{\mathbf{r}_i+\mathbf{r}} \rangle$ where $\delta\rho_{\mathbf{r}_i} = f_i^\dagger f_i - \rho_F$. We obtain $C(\mathbf{r}) = -n^2(\mathbf{r})$ where $n(\mathbf{r}) = (1/N) \sum_{\mathbf{k}} \langle f_{\mathbf{k}}^\dagger f_{\mathbf{k}} \rangle e^{i\mathbf{k}\cdot\mathbf{r}}$, and $C_{\mathbf{q}} = -(1/N) \sum_{\mathbf{k}} \langle f_{\mathbf{k}}^\dagger f_{\mathbf{k}} \rangle \langle f_{\mathbf{k}+\mathbf{q}}^\dagger f_{\mathbf{k}+\mathbf{q}} \rangle$ for the Fourier transform of $C(\mathbf{r})$ ^{38,39}. In our earlier work, we could show that $n(\mathbf{r})$ shows a periodicity of twice the lattice spacing for $\rho_F = 1/2$, while no apparent periodicity was obtained for other values of ρ_F . Using the expression for the Fermi function in Eq. (13), we can readily see that in the disordered phase ($\psi = 0$), we obtain $C_{\mathbf{q}} = -1/4$. This shows that there is no density wave (DW) order in

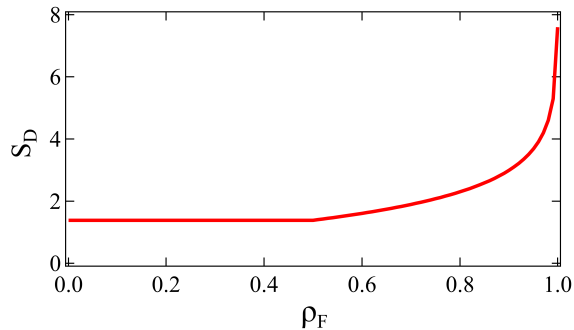


FIG. 1: The disordered-phase entropy $S_D = -\tilde{F}_D/T$ (equal to $-\tilde{F}_I/T$ for $\rho_F \leq 1/2$ and $-\tilde{F}_{II}/T$ for $\rho_F > 1/2$) plotted as a function of ρ_F . The high-temperature entropy is $2 \ln 2$, as expected, for $0 < \rho_F \leq 1/2$. However, it is anomalously high for $1/2 < \rho_F \leq 1$, the regime of zeroth-order transition.

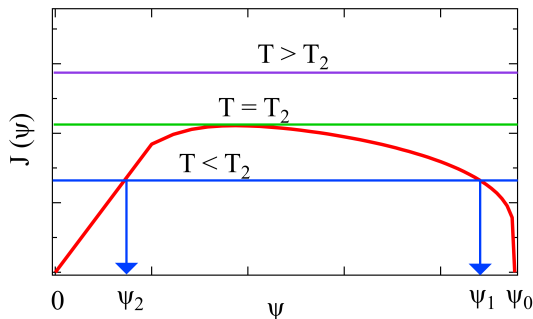


FIG. 2: A figure illustrating the graphical solution of the self-consistency equation $T = J(\psi)$. The function $J(\psi)$ vanishes at $\psi = 0, \psi_0$ and has a maximum in between. The horizontal lines show plots of $y = T$ (for $0 < T < T_2$, $T = T_2$, $T > T_2$). For $0 < T < T_2$, the line $y = T$ intersects the curve $y = J(\psi)$ (red curve) at two points $\psi = \psi_1, \psi_2$, with $\psi_0 \geq \psi_1 > \psi_2$, that correspond, respectively, to a minimum and a maximum of F . For $y = T_2$, the two points merge and the line is a tangent to the curve $J(\psi)$ at its maximum. For $T > T_2$, the self-consistency equation has no solution for any real value of ψ .

the insulating normal gas phase, and the DW order obtained for the $T = 0$ metallic superfluid^{38,39} is stabilized by the nesting of the Fermi surface and the superfluidity of the Bose sector.

IV. DISCUSSION

Our numerical results are presented in figures 1-8. In Fig.1 we show the behavior of disordered-phase entropy as a function of ρ_F . The entropy in this case is $S_D = -\tilde{F}_D/T$, where F_D is the disordered-phase free energy minimum. As we discussed above, this is $-\tilde{F}_I/T$ for $\rho_F \leq 1/2$ and $-\tilde{F}_{II}/T$ for $\rho_F > 1/2$. We can see that the

entropy is $2 \ln 2$ for $\rho_F \leq 1/2$ as one might expect in the disordered phase. However, the entropy is anomalously large for $\rho_F > 1/2$, which is also the regime where the temperature-driven transition is zeroth order. We believe this is a consequence of the filling constraint (1), that leads to the solution in equation (25) for α so that $\alpha = T[\ln(1 - \rho_F) - \ln \rho_F]$ in this case (see equation (26)).

To understand how temperature suppresses the metallic-superfluid order, we solve the self-consistency equations (24) and (25) for ψ , α using an approach graphically described in Fig.2. As shown in the figure, at a certain temperature $T < T_2$, the line $y = T$ intersects the curve $y = J(\psi)$ at two points ψ_1, ψ_2 ($\psi_0 \geq \psi_1 > \psi_2$). The solution $\psi = \psi_1$ corresponds to the free energy minimum at this temperature. As the temperature increases, it is obvious from the figure that this solution moves to the left, i.e. decreases, leading to a thermal suppression of superfluidity. At a certain high temperature $T > T_2$, the line $y = T$ has no intersection with the curve $y = J(\psi)$. Therefore there is no solution to the self-consistency equation $T = J(\psi)$ at temperatures higher than a certain T_2 , at which point the line $y = T$ becomes a tangent to the curve $y = J(\psi)$ at its maximum.

By numerically implementing this graphical method of solution, we can obtain ψ , ϕ , μ , \tilde{F} , α and S (the entropy) as the temperature T is varied; these results are plotted in panels (a)-(f) of Fig.3. Each panel shows temperature dependence of one of these quantities for five different values of $\rho_F = 0.35, 1/2, 0.70, 0.81, 0.95$. This choice of ρ_F values is the same as for the $T = 0$ case, which span the superfluid metallic phase as reported earlier^{38,39}. The figures show that at each of these fillings, there is a certain critical temperature T_c where the model has a discrete phase transition: the quantities ψ, ϕ, μ and α all show discontinuous changes at T_c (figures 3(a, b, c, e)). We can observe that at $\rho_F = 0.35$ and $1/2$, the free energy minimum \tilde{F} is continuous, but with a derivative discontinuity, whereas it is discontinuous at $\rho_F = 0.70, 0.81$ and 0.95 (Fig. 3(d)).

In figure 3(f) we show plots of entropy $S(T) = -\partial\tilde{F}/\partial T$, computed by numerical differentiation of $\tilde{F}(T)$. The unusual feature that can be readily seen is that the entropy becomes *negative* for certain temperatures below T_c when $\rho_F > 1/2$. While the concept of negative entropy has been applied to quantum information systems earlier^{54,55}, it's relevance for physical systems has been discussed only recently⁵⁶. Cerf and Adami showed that unlike in classical information theory, quantum conditional entropies can be negative for quantum entangled systems⁵⁴. Subsequently, del Rio et al. explained its thermodynamic meaning: negative entropy is related to a possible cooling of an environment connected to a quantum information system, when quantum information contained in the system is erased⁵⁵. In a very recent study⁵⁶, it has been proposed that the results of two independent inelastic neutron scattering experiments^{57,58}, which showed an anomalous scattering

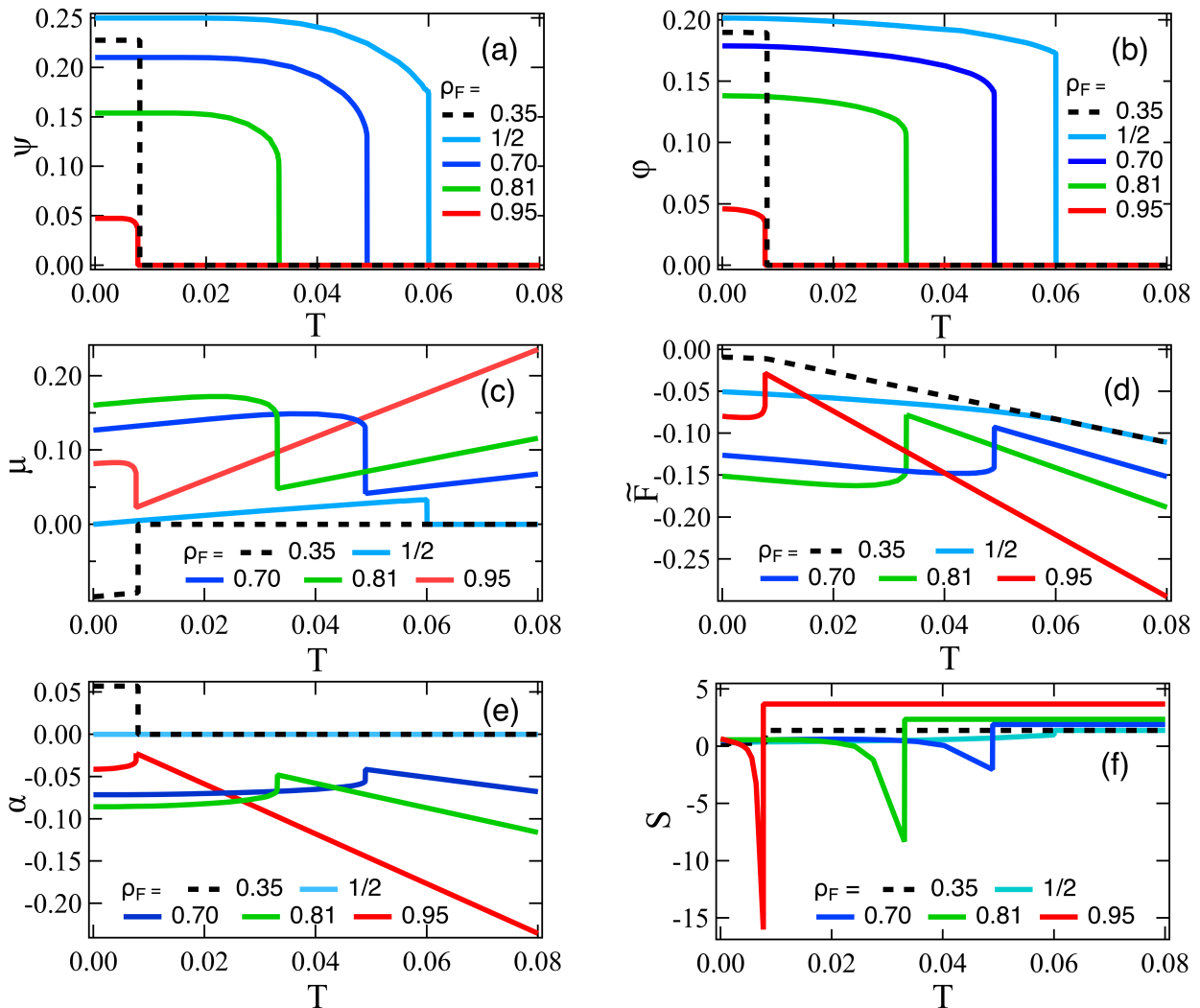


FIG. 3: Panels (a)-(f) show the T -dependence plots, respectively, of ψ , ϕ , μ , \tilde{F} , α and S . Each panel has plots at five different values of ρ_F , namely $0.35, 1/2, 0.70, 0.81, 0.95$.

from H_2 molecules in nanoscale confined geometries, can be explained on the basis of negative conditional entropy and quantum thermodynamics.

Our numerical results for $\rho_F \leq 1/2$ show that at $T = T_c = T_1$, the ordered and disordered phases coexist and we have $\tilde{F}_O = \tilde{F}_D$. The ordered minimum survives well into the disordered phase, and disappears at a temperature $T_2 > T_1$. We have therefore a standard first-order transition in this case. On the other hand, for $\rho_F > 1/2$, the ordered minimum disappears abruptly at a certain temperature $T_2(\rho_F)$. The system then assumes the only minimum available to it, namely the disordered minimum. The free energy obviously shows a discontinuous jump in this case. The transition is therefore zeroth order. These numerical results are consistent with the qualitative remarks we made above in Section III.

As a result, we can define T_1 only for $\rho_F \leq 1/2$, where

clearly $T_c = T_1 < T_2$. These results are summarized in figures 4 and 5. Figure 4 shows the phase diagram of our model in $\rho_F - T$ plane, showing the metallic superfluid under the dome, and two insulating non-superfluid phases outside it. We refer to the insulating phase at $T = 0$ for $0 < \rho_F < 0.3$ as an insulating normal liquid and the insulating phase for $T > 0$ as an insulating normal gas. While the latter is dominated by thermal effects, the former is an unusual phase of bosons at $T = 0$ that is a non-superfluid because of correlation and quantum effects.

Figure 5 shows the plots of $T_1(\rho_F)$ and $T_2(\rho_F)$. The function $T_2(\rho_F)$ can be defined for $0 \leq \rho_F \leq 1$, and has a maximum at a certain $\rho_F < 1/2$. The temperature T_1 on the other hand remains lower than T_2 ; it vanishes for $0 \leq \rho_F \leq 0.3$, in agreement with the $T = 0$ results^{38,39}.

The line separating the two phases in Fig. 4 has a

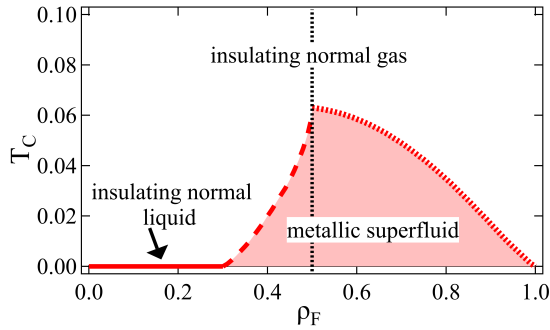


FIG. 4: The phase diagram of model (2) in (ρ_F, T) plane showing the metallic superfluid ($\phi, \psi > 0$) and insulating non-superfluid phases ($\phi = \psi = 0$) phases (the insulating normal liquid at $T = 0$ and the insulating normal gas for $T > 0$). These phases are separated by lines of discontinuous transitions: at the phase boundary, the minimum free energy \tilde{F} is continuous with a derivative discontinuity for $\rho \leq 1/2$ (first-order transition, dashed line), while \tilde{F} has a jump for $\rho > 1/2$ (zeroth-order transition, dotted line).

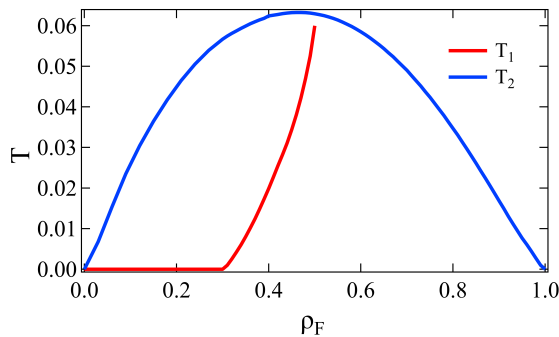


FIG. 5: The temperatures T_1 and T_2 are plotted as functions of ρ_F . As explained in the text, T_1 is the critical temperature for first-order transition, where $\tilde{F}_O = \tilde{F}_D$. It is not defined for $\rho_F > 1/2$, where $\tilde{F}_O < \tilde{F}_D$ for $T \leq T_2$. The ordered minimum disappears at T_2 . The critical temperature T_c is T_1 for $\rho_F \leq 1/2$ (first-order transition) and T_2 for $\rho_F > 1/2$ (zeroth-order transition). Note that $T_2 > T_1$. This is responsible for a segment of the phase boundary in Fig. 4 being vertical at $\rho_F = 1/2$.

vertical segment at the van Hove point $\rho_F = 1/2$. This is as a consequence of two facts: (a) T_c is the lower of T_1 and T_2 , and (b) $T_1 < T_2$, for $\rho_F \leq 1/2$.

As we saw in Fig.3, the superfluid order parameter ψ is discontinuous with a jump ψ_c at T_c . In Fig.6 we show the plot of $\psi_c^2(\rho_F)$. The jump in the order parameter seems to be maximum around the same ρ_F where $T_2(\rho_F)$ is maximum. It shows an abrupt drop at $\rho_F = 1/2$, and after a broad maximum, decreases slowly towards zero at $\rho_F = 1$.

Based on the zero-temperature Fermi band width of $B_0 = 2\psi_0^2$, the ratio T_c/B_0 agreed very well with measured values for several types of unconventional super-

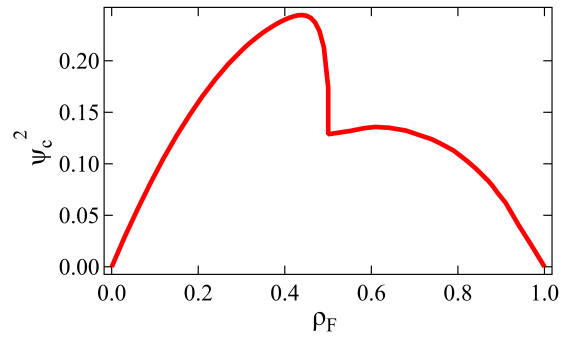


FIG. 6: Plot of ψ_c^2 , where ψ_c is the jump in the superfluid order parameter at the discontinuous transition temperature T_c , as a function of ρ_F .

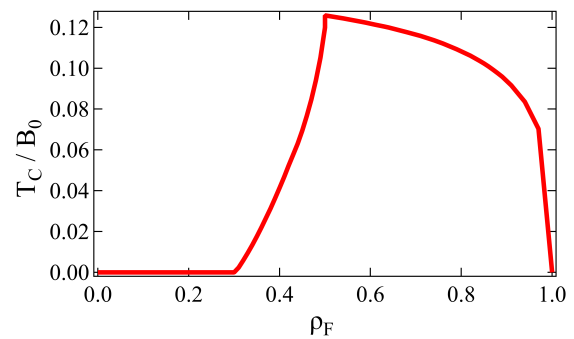


FIG. 7: Plot of T_c/B_0 as a function of ρ_F . Here, $B_0 = 2\psi_0^2$ is the Fermi band width at $T = 0$ ^{38,39}.

fluids and superconductors in our earlier work^{38,39}. This value of $T_c \simeq 0.12$ in our earlier work was not based on a calculation, but only an estimate based on the zero-temperature free energy minimum for $\rho_F = 1/2$. However, in our present work we have performed explicit computation of T_c based on T_1, T_2 calculations for the whole range of ρ_F from 0 to 1, as shown in figures (4) and (5). Figure 7 presents a plot of the ratio T_c/B_0 as a function

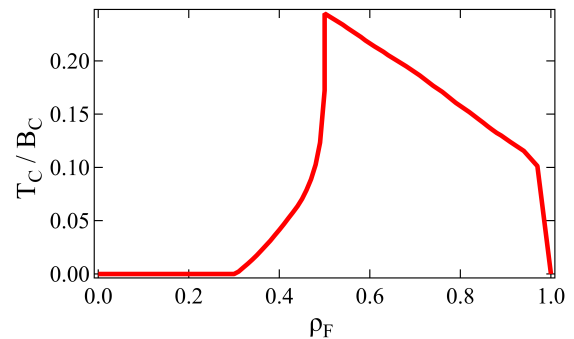


FIG. 8: Plot of T_c/B_c as a function of ρ_F . Here, $B_c = 2\psi_c^2$ is the $T = T_c$ analogue of the $T = 0$ Fermi band widths B_0 .

of ρ_F . We note that the calculated value of the ratio for $\rho_F = 1/2$ is in almost exact agreement with our earlier estimate^{38,39}. The ratio is between 0.01 and 0.10 for most ρ_F values in the range 0.3 to 1.0.

Figure 8 plots the ratio T_c/B_c as a function of ρ_F , using $B_c = 2\psi_c^2$, the $T = T_c$ analogue of the $T = 0$ Fermi band width B_0 . It is interesting to compare this with experimentally determined values of the ratio T_c/T_F , of the superfluid or superconducting transition temperature T_c to the Fermi temperature T_F . This ratio also scales approximately with the ratio Δ/E_F , the pairing strength of single-band superconductors, where Δ is the superconducting gap and E_F is the Fermi energy. In particular, it has been recognized⁵⁹ that the unconventional superconductors show a relatively large value of $T_c/T_F \sim 0.02 - 0.2$, while the conventional superconductors show a small value of $T_c/T_F \sim 10^{-4}$ to 10^{-5} . For example, elemental metal tin (Sn)⁶⁰ has a $T_c/T_F \sim 3 \times 10^{-5}$, while the high- T_c -cuprates⁶¹⁻⁶³ exhibit a $T_c/T_F \sim 0.02-0.03$. On the other hand, the iron based superconductors (estimated from experimental data^{5-8,64}) and the newly discovered hydride superconductors (as estimated from experimental T_c values⁶⁵⁻⁶⁷ and band structure calculations⁶⁸⁻⁷⁰) show $T_c/T_F \sim 0.1 - 0.2$. Surprisingly, the corresponding value for a Fermi-Bose mixture⁷¹ estimated from experimental data is $T_c/T_F \simeq 0.19$, although the $T_c \sim 200$ nK. Even for a purely ultracold Fermi atomic system⁷², $T_c/T_F \simeq 0.2$. Thus, the high- T_c cuprates, iron-based superconductors, hydrides and ultracold atomic systems are clearly classified as unconventional superconductors/superfluids⁷³.

A very recent study on an iron-based superconductor has reported evidence for the first solid-state BEC superconductor, although the observed value of the ratio Δ/E_F ($\simeq 0.12$, corresponding to a $T_c/T_F \simeq 0.025$) is reduced across the BCS-BEC crossover, and the authors interpret it as most probably arising from interband coupling effects⁷⁴.

The T_c values of these unconventional materials span nine orders of magnitude: while the ultracold FBMs have $T_c \simeq 200$ nK, the hydrides have a $T_c \simeq 250$ K. But the important point is that the ratio calculated in our model is remarkably close to these values for several classes of unconventional superfluids and superconductors. In particular, we obtain $T_c/B_0 \sim 0.01 - 0.1$ ($T_c/B_c \sim 0.01 - 0.25$); the value of this ratio is a very robust feature of our model, and compares well with the range $0.03 - 0.22$ for most unconventional materials (see the Table 1 of our previous paper for details³⁹).

An important question is that of a potential experimental realization of the composite hopping model. Consider a lattice with N sites and M electrons ($2N > M > N$) with nearest-neighbor hopping and on-site repulsion. In this case, by the Pigeonhole principle, at least one site must have more than one electron. Taking into account the repulsion between electrons, in the minimum energy configuration we have $M - N$ local pairs (that can be considered as hardcore bosons) and $2N - M$ elec-

trons each occupying a site. When one of the electrons of a pair hops to a neighboring site with one electron, we have a realization of composite hopping (see our earlier work^{38,39} for a more detailed explanation). This situation is perhaps also well described by a one-band fermion Hubbard model above half filling, and the composite hopping model might offer a good effective description. Our model approximates the electrons by spinless fermions, but in subsequent work we plan to treat the spin half case. In this case, the composite hopping strength t is just the single-electron hopping strength. For a narrow band Hubbard model, we can take $t \sim 0.1 - 0.2$ eV, and if we further use $T_c \simeq 0.06zt$ (corresponding to its peak value in Fig.4 at the van Hove point $\rho_F = 1/2$), we obtain a value of $T_c \simeq 250 - 500$ K.

If room-temperature superconductivity is theoretically possible within a composite-hopping framework, then it provides a strong reason to look for practical examples of it. In the pigeonhole context discussed above, external pressure might help overcome the repulsion between electrons and keep them paired. It is interesting to explore if high-pressure room-temperature superconductors like sulphides⁷⁸ are indeed solid-state realizations of the composite-hopping model, and are superconducting because of such a ‘pigeonhole’ pairing mechanism.

A second possibility might be realization of composite hopping in the context of ultracold atoms in an optical lattice. Quantum simulation is an exciting area of research⁷⁵, and given the many unusual physical properties displayed by our model such as negative compressibility (discussed in our earlier work^{38,39}), negative entropy⁵⁴⁻⁵⁶, zeroth-order transition^{47-53,77} and the remarkable agreement of the calculated ratio of T_c/T_F with a wide range of unconventional superfluids and superconductors³⁹, it would be interesting to explore the physics of composite hopping in this perspective.

In our model, there is a clear distinction between the boson-dominated ($\rho_F \leq 1/2$) and the fermion-dominated ($\rho_F > 1/2$) regimes: in the former, the temperature-driven transition is first-order and the entropy remains positive throughout, while in the latter regime the transition is zeroth order and the entropy is negative in the ordered phase close to T_c . In the latter regime, the zero-temperature bulk modulus becomes negative over a range of ρ_F ³⁹.

An important question whether the zeroth order temperature-driven transition for $\rho_F > 1/2$ is a consequence of mean-field approximation (3), or an inherent property of the composite-hopping model. This question assumes importance given that the model offers an irreducible nontrivial description of an FBM perhaps not explored before, and the circumstance that zeroth-order transitions are relatively rare in the solid state^{47,77}. It would therefore be of interest to study the model using other numerical techniques of quantum many-body theory like Quantum Monte-Carlo calculations (QMC)⁷⁹.

V. CONCLUSION

In this work, we have extended the zero-temperature study of the composite hopping model of FBMs to explore finite-temperature thermodynamics. We computed the $\rho_F - T$ phase diagram and found that the temperature-driven metallic superfluid phase to insulating normal phase transition is discontinuous: for $\rho \leq 1/2$, it is first order, while for $\rho > 1/2$ it is zeroth order. We calculated the the temperature dependent superfluid amplitude ψ , the fermion hopping amplitude ϕ , the Fermi chemical potential, and free energy within a mean-field approximation. We also computed the entropy and found that it becomes negative for a certain range of temperatures below T_c when $\rho_F > 1/2$. The ratios T_c/B_0 and T_c/B_c where B_0 and B_c are Fermi band widths at $T = 0$

and $T = T_c$, respectively, could also be calculated. The calculated ratios of T_c to Fermi band widths match well with experimental values of T_c/T_F (where T_F is the Fermi temperature) of unconventional superfluids and superconductors, including Fermi-Bose mixtures, the high- T_c cuprates and iron-based superconductors, that span a T_c range of nine orders. The results indicate the important role of composite hopping in describing the superfluid properties of Fermi-Bose mixtures.

Acknowledgments

A.C. thanks the Ministry of Science and Technology of the Republic of China, Taiwan, for financially supporting this research under Contract No. MOST 108-2112-M-213-001- MY3.

* Electronic address: kshesh@gmail.com

† Electronic address: chainania@gmail.com

¹ C. Ebner and D. O. Edwards, “The low temperature thermodynamic properties of dilute solutions of ^3He in ^4He ”, *Phys. Rep.* 2, 77 (1970).

² A. G. Truscott, K. E. Strecker, W. I. McAlexander, G. B. Patridge, and R. G. Hulet, “Observation of Fermi Pressure in a Gas of Trapped Atoms”, *Science* 291, 2570 (2001).

³ F. Schreck, L. Khaykovich, K.L. Corwin, G. Ferrari, T. Bourdel, J. Cubizolles, and C. Salomon, “Quasipure Bose-Einstein Condensate Immersed in a Fermi Sea”, *Phys. Rev. Lett.* 87, 080403 (2001).

⁴ Z. Hadzibabic, C.A. Stan, K. Dieckmann, S. Gupta, M.W. Zwierlein, A. Gorlitz, and W. Ketterle, “Two-Species Mixture of Quantum Degenerate Bose and Fermi Gases”, *Phys. Rev. Lett.* 88, 160401 (2002).

⁵ Y. Lubashevsky, E. Lahoud, K. Chashka, D. Podolsky, and A. Kanigel, “Shallow pockets and very strong coupling superconductivity in $\text{FeSe}_x\text{Te}_{1-x}$ ”, *Nat Phys* 8, 309 (2012).

⁶ K. Okazaki, Y. Ito, Y. Ota, Y. Kotani, T. Shimojima, T. Kiss, S. Watanabe, C. -T. Chen, S. Niitaka, T. Hanaguri, H. Takagi, A.Chainani, and S. Shin, “Superconductivity in an electron band just above the Fermi level: possible route to BCS-BEC superconductivity”, *Sci. Rep.* 4, 4109; DOI:10.1038/srep04109 (2014).

⁷ Shigeru Kasahara, Tatsuya Watashige, Tetsuo Hanaguri, Yuhki Kohsaka, Takuya Yamashita, Yusuke Shimoyama, Yuta Mizukami, Ryota Endo, Hiroaki Ikeda, Kazushi Aoyama, Taichi Terashima, Shinya Uji, Thomas Wolf, Hilbert von Lohneysen, Takasada Shibauchi, and Yuji Matsuda, “Field-induced superconducting phase of FeSe in the BCS-BEC cross-over”, *PNAS*, 111, 16311 (2014).

⁸ Shahar Rinott, K. B. Chashka, Amit Ribak, Emile D. L. Rienks, Amina Taleb-Ibrahimi, Patrick Le Fevre, Francois Bertran, Mohit Randeria and Amit Kanigel, “Tuning across the BCS-BEC crossover in the multiband superconductor $\text{Fe}_{1+y}\text{Se}_x\text{Te}_{1-x}$: An angle-resolved photoemission study”, *Science Advances* 3, e1602372 DOI: 10.1126/sciadv.1602372.

⁹ C. A. Regal, C. Ticknor, J. L. Bohn, and D. S. Jin, “Tuning p-wave interactions in an ultracold Fermi gas of atoms”, *Phys. Rev. Lett.* 90, 053201 (2003).

¹⁰ M. Randeria and E. Taylor, “Crossover from Bardeen-Cooper-Schrieffer to Bose-Einstein condensation and the unitary Fermi gas”, *Annual Review of Condensed Matter Physics* 5, 209 (2014).

¹¹ W. Ketterle and M. W. Zwierlein, in *Proceedings of the International School of Physics: Enrico Fermi*, edited by M. Inguscio, W. Ketterle, and C. Salomon (IOS Press, 2008) pp.95-287.

¹² L. V. Keldysh and A. N. Kozlov, “Collective properties of excitons in semiconductors,” *Sov. Phys. JETP* 27, 521 (1968).

¹³ B. O. Kerbikov, “BCS-Bose crossover in color superconductivity,” *Phys. At. Nucl.* 65, 1918 (2002), arXiv:hep-ph/0204209.

¹⁴ M. Bartenstein, A. Altmeyer, S. Riedl, S. Jochim, C. Chin, J. Hecker Denschlag, and R. Grimm, “Crossover from a molecular Bose-Einstein condensate to a degenerate Fermi gas”, *Phys. Rev. Lett.* 92, 120401 (2004).

¹⁵ Tyler D. Cumby, Ruth A. Shewmon, Ming-Guang Hu, John D. Perreault, and Deborah S. Jin, “Feshbach molecule formation in a Bose Fermi mixture”, *Phys. Rev. A* 87, 012703.

¹⁶ Ruth S. Bloom, Ming-Guang Hu, Tyler D. Cumby, and Deborah S. Jin, “Tests of Universal Three Body Physics in an Ultracold Bose-Fermi Mixture”, *Phys. Rev. Lett.* 111, 105301 (2013).

¹⁷ M. Randeria, J.-M.Duan, and L.-Y. Shieh, “Bound states, Cooper pairing, and Bose condensation in two dimensions”, *Phys. Rev. Lett.* 62, 981 (1989).

¹⁸ R. M. Quick, C. Eсеbbag, and M. De Llano. “BCS theory tested in an exactly solvable fermion fluid.” *Physical Review B* 47, 11512 (1993).

¹⁹ M. J. Bijlsma, B. A. Heringa and H. T. C. Stoof, “Phonon exchange in dilute Fermi-Bose mixtures: Tailoring the Fermi-Fermi interaction”, *Phys. Rev. A* 61, 053601 (2000).

²⁰ P. Capuzzi and E. S. Hernandez, “Phase separation and response of ^3He - ^4He mixtures within a magnetic trap”, *Phys. Rev. A* 64, 043607 (2001).

²¹ A. P. Albus, S. A. Gardiner, F. Illuminati, and M. Wilkens, “Quantum field theory of dilute homogeneous Bose-Fermi mixtures at zero temperature: General formalism and beyond mean-field corrections”, *Phys. Rev. A* 65, 053607

- (2002).
- 22 L. Viverit and S. Giorgini, Ground-state properties of a dilute Bose-Fermi mixture, *Phys. Rev. A* 66, 063604 (2002).
 - 23 M. R. Schafroth, “Theory of superconductivity”, *Phys. Rev.* 96, 1442 (1954).
 - 24 J. Ranninger and S. Robaszkiewicz, “Superconductivity of locally paired electrons”, *Physica B* 135, 468 (1985).
 - 25 J. Ranninger, J. M. Robin, and M. Eschrig, “Superfluid precursor effects in a model of hybridized bosons and fermions”, *Phys. Rev. Lett.* 74, 4027 (1995).
 - 26 R. Friedberg and T. D. Lee, “Gap energy and long-range order in the boson-fermion model of superconductivity”, *Phys. Rev. B* 40, 6745 (1989).
 - 27 V. B. Geshkenbein, L. B. Ioffe, and A. I. Larkin, “Superconductivity in a system with preformed pairs”, *Phys. Rev. B* 55, 3173 (1997).
 - 28 T. Domanski, M. M. Maska, and M. Mierzejewski, “Upward curvature of the upper critical field in the boson-fermion model”, *Phys. Rev. B* 67, 134507 (2003).
 - 29 Y.-I. Shin, C. H. Schunck, A. Schirotzek, and W. Ketterle, “Phase diagram of a two-component Fermi gas with resonant interactions”, *Nature* 451, 689 (2008).
 - 30 M. M. Maska and N. Trivedi, “Temperature-driven BCS-BEC crossover and Cooper-paired metallic phase in coupled boson-fermion systems”, *Phys. Rev. B* 102, 144506 (2020).
 - 31 Christian Ufrecht, Matthias Meister, Albert Roura and Wolfgang P. Schleich, “Comprehensive classification for Bose-Fermi mixtures”, *New J. Phys.* 19, 085001 (2017).
 - 32 C. Ospelkaus, S. Ospelkaus, K. Sengstock and K. Bongs, Interaction-driven dynamics of ^{40}K - ^{87}Rb fermion-boson gas mixtures in the large-particle-number limit, *Phys. Rev. Lett.* 96 020401 (2006) ; S. Ospelkaus, C. Ospelkaus, L. Humbert, K Sengstock and K. Bongs, “Tuning of heteronuclear interactions in a degenerate Fermi-Bose mixture”, *Phys. Rev. Lett.* 97 120403 (2007)
 - 33 X.-W. Guan, M. T. Batchelor, and J.-Y. Lee, “Magnetic ordering and quantum statistical effects in strongly repulsive Fermi-Fermi and Bose-Fermi mixtures”, *Physical Review A* 78, 023621 (2008).
 - 34 D. W. Wang, M. D. Lukin, and E. Demler, “Engineering superfluidity in Bose-Fermi mixtures of ultracold atoms”, *Phys. Rev. A* 72, 051604 (2005).
 - 35 M. Cramer, “Interaction-Dependent Temperature Effects in Bose-Fermi Mixtures in Optical Lattices”, *Phys. Rev. Lett.* 106, 215302 (2011).
 - 36 M. Lewenstein, L. Santos, M. A. Baranov and H. Fehrmann, “Atomic Bose-Fermi mixtures in an optical lattice”, *Phys. Rev. Lett.* 92, 050401 (2004).
 - 37 L. Pollet, M. Troyer, K. Van Houcke, and S. M. A. Rombouts, “Phase diagram of Bose-Fermi mixtures in one-dimensional optical lattices”, *Phys. Rev. Lett.* 96, 190402 (2006).
 - 38 K. Sheshadri and A Chainani, “A Composite-Hopping Model of Fermi-Bose Mixtures”, arxiv/1912.00132 (2019).
 - 39 K Sheshadri and A Chainani, “Coupled first-order transitions and unconventional superfluidity in a Fermi-Bose mixture”, *Physical Review Research* 2 (2), 023291 (2020).
 - 40 K. Sheshadri, H. R. Krishnamurthy, R Pandit and T. V. Ramakrishnan, “Superfluid and Insulating Phases in an Interacting-Boson Model: Mean-Field Theory and the RPA. *Europhys. Lett.*, 22, 267 (1993).
 - 41 K. Sheshadri, H. R. Krishnamurthy, Rahul Pandit, and T. V. Ramakrishnan, “Percolation-Enhanced Localization in the Disordered Bosonic Hubbard Model”, *Phys. Rev. Lett.* 75, 4075 (1995).
 - 42 Matthew P. A. Fisher, Peter B. Weichman, G. Grinstein, and Daniel S. Fisher, “Boson localization and the superfluid-insulator transition”, *Phys. Rev. B* 40, 546 (1989).
 - 43 W. Krauth, M. Caffarel, J. P. Bouchaud, “Gutzwiller wave function for a model of strongly interacting bosons”, *Physical Review B* 45, 3137 (1992).
 - 44 R. V. Pai, K. Sheshadri, R. Pandit, “Phases and transitions in the spin-1 Bose-Hubbard model: Systematics of a mean-field theory”, *Physical Review B* 77, 014503 (2008).
 - 45 R. V. Pai, J. M. Kurdestany, K. Sheshadri, R. Pandit, “Bose-Hubbard models in confining potentials: Inhomogeneous mean-field theory”, *Physical Review B* 85, 214524 (2012).
 - 46 Takashi Kimura, Shunji Tsuchiya, and Susumu Kurihara, “Possibility of a First-Order Superfluid Mott-Insulator Transition of Spinor Bosons in an Optical Lattice”, *Phys. Rev. Lett.* 94, 110403 (2005).
 - 47 V.P. Maslov, “Zeroth-Order Phase Transitions”, *Mathematical Notes* 76, 697 (2004).
 - 48 S. Gunasekaran, R. B. Mann and D. Kubiznak, *JHEP* 11, 110 (2012).
 - 49 N. Altamirano, D. Kubiznak, and R. B. Mann, *Phys. Rev. D.* 88, 101502(R) (2013); N. Altamirano, D. Kubiznak, R. B. Mann and Z. Sherkatghanad, *Class. Quant. Grav.* 31, 042001 (2014); S. W. Wei, P. Cheng and Y. X. Liu, *Phys. Rev. D* 93, 084015 (2016).
 - 50 D. Zou, Y. Liu, B. Wang, *Phys. Rev. D.* 90, 044063 (2014); R. A. Hennigar, W. G. Brenna and R. B. Mann, *JHEP* 1507, 077 (2015); M. B. Jahani Poshteh, B. Mirza, Z. Sherkatghanad, *Phys. Rev. D* 88, 024005 (2013).
 - 51 R. A. Hennigar and R. B. Mann, *Entropy* 17, 8056 (2015).
 - 52 N. Altamirano, D. Kubiznak, R. B. Mann and Z. Sherkatghanad, *Galaxies* 2, 89 (2014); D. Kubiznak and F. Simovic, *Class. Quant. Grav.* 33, 245001 (2016).
 - 53 Amin Dehyadegari and Ahmad Sheykhi, Reentrant phase transition of Born-Infeld-AdS black holes, *Phys. Rev. D* 98, 024011 (2018).
 - 54 N. J. Cerf and C. Adami, “Negative Entropy and Information in Quantum Mechanics”, *Phys. Rev. Lett.* 79, 5194 (1997).
 - 55 Lidia del Rio, Johan Aberg, Renato Renner, Oscar Dahlsten and Vlatko Vedral “The thermodynamic meaning of negative entropy”, *Nature* 474, 61-63 (2011).
 - 56 C. A. Chatzidimitriou-Dreismann, “Experimental Implications of Negative Quantum Conditional Entropy – H2 Mobility in Nanoporous Materials”, *Applied Sciences* 10, 8266 (2020) ; doi:10.3390/app10228266.
 - 57 Raina J. Olsen, Matthew Beckner, Matthew B. Stone, Peter Pfeifer, Carlos Wexler, and Haskell Taub, “Quantum excitation spectrum of hydrogen adsorbed in nanoporous carbons observed by inelastic neutron scattering”, *Carbon*, 58, 46 (2013).
 - 58 Samantha K. Callear, Anibal J. Ramirez-Cuesta, William I.F. David, Franck Millange, Richard I. Walton, “High-resolution inelastic neutron scattering and neutron powder diffraction study of the adsorption of dihydrogen by the Cu(II) metal-organic framework material HKUST-1”, *Chemical Physics* 427, 9 (2013).
 - 59 Y. J. Uemura, “Basic similarities among cuprate, bismuthate, organic, chevre-phase and heavy-fermion superconductors shown by penetration-depth measurements”

- Phys. Rev. Lett. 66 2665 (1991) ; “Condensation, excitation, pairing, and superfluid density in high-Tc superconductors: the magnetic resonance mode as a roton analogue and a possible spin-mediated pairing”, J. Phys.: Condens. Matter 16, S4515 (2004).
- ⁶⁰ N. W. Ashcroft and N. D. Mermin, Solid State Physics, Saunders College Publishing, Florida (1975).
- ⁶¹ A. Yamamoto, N. Takeshita, C. Terakura, and Y. Tokura, “High pressure effects revisited for the cuprate superconductor family with highest critical temperature”, Nat. Commun. 6, 8990 (2015).
- ⁶² N. B. Brookes, G. Ghiringhelli, O. Tjernberg, L. H. Tjeng, T. Mizokawa, T. W. Li, and A. A. Menovsky, “Detection of Zhang-Rice Singlets Using Spin-Polarized Photoemission”, Phys. Rev. Lett. 87, 237003 (2001).
- ⁶³ B. P. Xie, K. Yang, D. W. Shen, J. F. Zhao, H. W. Ou, J. Wei, S. Y. Gu, M. Arita, S. Qiao, H. Namatame, M. Taniguchi, N. Kaneko, H. Eisaki, Z. Q. Yang, D.L. Feng, “High-energy scale revival and giant kink in the dispersion of a cuprate superconductor”, Phys. Rev. Lett. 98, 147001 (2007).
- ⁶⁴ Q. Song, T.L. Yu, X. Lou, B.P. Xie, H.C. Xu, C.H.P. Wen, Q. Yao, S.Y. Zhang, X.T. Zhu, J.D. Guo, R. Peng and D.L. Feng, “Evidence of cooperative effect on the enhanced superconducting transition temperature at the FeSe/SrTiO₃ interface”, Nat. Commun.10, 758 (2019), doi.org/10.1038/s41467-019-08560-z.
- ⁶⁵ A. P. Drozdov, M. I. Erements, I. A. Troyan, V. Ksenofontov and S. I. Shylin, “Conventional superconductivity at 203 kelvin at high pressures in the sulfur hydride system”, Nature 525, 73 (2015).
- ⁶⁶ A. P. Drozdov, P. P. Kong, V. S. Minkov, S. P. Besedin, M. A. Kuzovnikov, S. Mozaffari, L. Balicas, F. F. Balakirev, D. E. Graf, V. B. Prakapenka, E. Greenberg, D. A. Knyazev, M. Tkacz and M. I. Erements, “Superconductivity at 250 K in lanthanum hydride under high pressures”, Nature 569, 528 (2019).
- ⁶⁷ Evidence for Superconductivity above 260 K in Lanthanum Superhydride at Megabar Pressures M. Somayazulu, M. Ahart, A. K. Mishra, Z. M. Geballe, M. Baldini, Y. Meng, V. V. Struzhkin, and R. J. Hemley, “Evidence for Superconductivity above 260 K in Lanthanum Superhydride at Megabar Pressures”, Phys. Rev. Lett. 122, 027001 (2019).
- ⁶⁸ A. Bianconi and T. Jarlborg, “Superconductivity above the lowest Earth temperature in pressurized sulfur hydride”, EPL (Europhysics Letters) 112, 37001 (2015).
- ⁶⁹ T. Jarlborg and A. Bianconi, “Breakdown of the Migdal approximation at Lifshitz transitions with giant zero-point motion in the H₃S superconductor”, Sci. Rep. 6, 24816; doi: 10.1038/srep24816 (2016).
- ⁷⁰ H. Liu , I. I. Naumov , R. Hoffmann , N. W. Ashcroft, and R. J. Hemley, “Potential high-Tc superconducting lanthanum and yttrium hydrides at high pressure”, PNAS 114, 6990 (2017).
- ⁷¹ I. Ferrier-Barbut, M. Delehaye, S. Laurent, A. T. Grier, M. Pierce, B. S. Rem, F. Chevy, C. Salomon, “A mixture of Bose and Fermi superfluids”, Science 345, 1035 (2014).
- ⁷² C. Chin, M. Bartenstein, A. Altmeyer, S. Riedl, S. Jochim, J. Hecker Denschlag, R. Grimm, “Observation of the Pairing Gap in a Strongly Interacting Fermi Gas”, Science 305, 1128 (2004).
- ⁷³ Yonko T Millev and Dimo I Uzunov, “Weakly First-Order Transition in Unconventional Superconductors”, Phys. Lett. A 145, 287 (1990).
- ⁷⁴ T. Hashimoto, Y. Ota, A. Tsuzuki, T. Nagashima, A. Fukushima, S. Kasahara , Y. Matsuda , K. Matsuura , Y. Mizukami , T. Shibauchi, Shik Shin, K. Okazaki, “Bose-Einstein condensation superconductivity induced by disappearance of the nematic state”, Sci. Adv. 2020; 6 : eabb9052.
- ⁷⁵ Maciej Lewenstein, Anna Sanpera, and Veronica Ahufinger, “Ultracold Atoms in Optical Lattices: Simulating quantum many-body systems”, Oxford University Press (2012).
- ⁷⁶ V.P. Maslov, “Zeroth-Order Phase Transitions”, Mathematical Notes 76, 697 (2004).
- ⁷⁷ Satyaki Kundu, Tapas Bar, Rajesh Kumble Nayak, and Bhavtosh Bansal, “Critical Slowing Down at the Abrupt Mott Transition: When the First-Order Phase Transition Becomes Zeroth Order and Looks Like Second Order”, Phys. Rev.Lett. 124, 095703 (2020).
- ⁷⁸ Elliot Snider, Nathan Dasenbrock-Gammon, Raymond McBride, Mathew Debessai, Hiranya Vindana, Kevin Venkatasamy, Keith V. Lawler, Ashkan Salamat and Ranga P. Dias, “Room-temperature superconductivity in a carbonaceous sulfur hydride”, Nature 586, 373 (2020).
- ⁷⁹ Werner Krauth and Nandini Trivedi, “Mott and superfluid transitions in a strongly interacting lattice boson system.” EPL (Europhysics Letters) 14, 627 (1991).